Royal Norwegian Council
for Scientific and Industrial Research
(NTNF)

NORSAR

NORSAR Scientific Report No. 2-92/93

Semiannual Technical Summary

1 October 1992 — 31 March 1993

Kjeller, July 1993

7.5 Initial processing results from the Spitsbergen small-aperture array

During the fall of 1992, a new regional array was installed near the town of Longyearbyen on the Arctic island of Spitsbergen (see Mykkeltveit et al, 1992). Fig. 7.5.1 shows the location of this array and Fig. 7.5.2 shows the array geometry. As of early 1993, six of the nine array sites had been finalized, and this study is based on these six instruments.

In the following we report on some initial results from analyzing data from the new array. It is emphasized that these results are preliminary, since the available data cover only a few months, and only a partial array has been installed until now. Thus a more comprehensive assessment must await the collection of more complete array data over a longer time span.

Noise spectra

Fig. 7.5.3a shows an example of corrected noise spectra for the 6 vertical elements of the Spitsbergen array, taken at 00.00 hours (GMT) on day 345, 1992. For comparison, the ARCESS spectra for the same number of channels and taken at the same time are shown in Fig. 7.5.3b. From these figures, it is seen that the Spitsbergen array has practically the same noise level as ARCESS, especially for the "best" Spitsbergen sensor (B2). However, the Spitsbergen array has a much larger variation in noise level than ARCESS, especially at low frequencies.

Fig. 7.5.4a shows 41 corrected noise spectra, taken daily at 00.00 GMT during the period 10 December 1992 - 18 January 1993 for the Spitsbergen array (instrument B2). These spectra represent typical winter conditions. For comparison, a similar set of spectra during summer (23 May - 7 June) is shown in Fig. 7.5.4.b. The range is similar for the two time periods, although the highest noise levels at low frequencies are observed during winter.

Noise suppression

Previous studies have shown that regional arrays are very effective in suppressing seismic noise, thus providing gains that are often of the order of $\sqrt{N}$, or sometimes even in excess of this value (N being the number of sensors). Such better than $\sqrt{N}$ suppression occurs when particular subgeometries are chosen, enhancing the suppression of noise at certain frequencies. As a first check on the capabilities of the Spitsbergen array in this regard, we have computed noise suppression curves for the initial array geometry.

We calculate an uncorrected power density spectrum first by prewhitening 60 seconds of data. Then we estimate the autocorrelation for 6 partially overlapping windows (window length 12 seconds), and compute power density spectra from the average autocorrelation, with compensation for the prewhitening filter.

An average spectrum is obtained by averaging the individual channel spectra for the array. The averaging is done after a logarithmic transform of the spectra, and the standard deviation for each frequency point is calculated. Each spectrum is pointwise compared to the average spectrum. If a value is outside 1.5 standard deviation from the mean value, the point is considered an outlier. If a single channel spectrum has more than 60% outliers, the spectrum is excluded and a new average spectrum is estimated. A beam is calculated using only those channels for which the spectrum was accepted. The suppression is then the beam spectrum divided by the average spectrum.

Fig. 7.5.5 shows noise suppression in the frequency range 0-20 Hz for an infinite-velocity beam (no time delays) for the Spitsbergen array. The figure shows an average of 24 noise samples, taken hourly on day 345, 1992. We note that the noise suppression is between 5 and 10 dB above 2 Hz. This is about the theoretical value (8 dB for 6 sensors). We anticipate further investigations into this subject after the full array is deployed.

Detection processing

Since the array was installed, the Spitsbergen data have been subjected to continuous on-line detection processing (DP) at NORSAR using the standard small-array detection algorithm. The initial beam deployment is shown in Table 7.5.1.

As an example of a regional seismic event recorded and processed using Apatity data, we show here results for a low-magnitude earthquake ($m_b \sim 2.0$) west of the array (on the North Atlantic Ridge).

Fig. 7.5.6 shows individual recordings for this event. Note the large variations in signal amplitudes across the array. In particular, the B2 instrument shows excellent signal-to-noise ratio for this event as well as for other events we have processed. The reason for this large amplitude variation is as yet unknown. There are two distinct P-onsets and one clear S-onset on the waveforms.

Frequency-wavenumber analysis

Frequency-wavenumber solutions for P and S are shown in Fig. 7.5.7. In spite of the small aperture of the array and the incomplete deployment, the peaks in the F-K diagram are well-defined. However, there is a tendency to side lobes in the plots.

From Fig. 7.5.7 we note that the phase velocities of each of the two phases are reasonably consistent with the phase type, the S phase having the slowest velocity. The estimated azimuths are quite consistent (256 and 260 degrees, respectively).

In conclusion, our preliminary analysis indicates that the Spitsbergen array will be an important supplement to the seismic array network in Northern Europe. Its inclusion into the Intelligent Monitoring System (IMS) will in particular serve to improve the location precision and source characterization of the large number of events in the Barents Sea and adjacent regions. The excellent recordings of this array from the small Novaya Zemlya event on 31 Dec 1992 (see subsection 7.4) is a further illustration of this point. Further

evaluation of the array capabilities will be made after the 9-element array has been completed.

J. Fyen
F. Ringdal

References

Mykkeltveit, S., A. Dahle, J. Fyen, T. Kværna, P.W. Larsen, R. Paulsen, F. Ringdal and I. Kuzmin (1992): Extensions of the Northern Europe Regional Array Network -- New small-aperture arrays at Apatity, Russia, and on the Arctic island of Spitsbergen, Semiannual Tech. Summ., 1 April - 30 September 1992, Scientific Rep. No. 1-92/93, NORSAR, Kjeller, Norway.

BEAM	Velocity	Azimuth	Filter band	Threshold	N	Configuration
S011	99999.9	0.0	0.5 - 1.5	4.4	6	A0B
S021	99999.9	0.0	1.0 - 3.0	4.4	6	A0B
S031	99999.9	0.0	1.5 - 3.5	4.4	6	A0B
S032	11.0	30.0	1.5 - 3.5	4.4	6	A0B
S033	11.0	90.0	1.5 - 3.5	4.4	6	A0B
S034	11.0	150.0	1.5 - 3.5	4.4	6	A0B
S035	11.0	210.0	1.5 - 3.5	4.4	6	A0B
S036	11.0	270.0	1.5 - 3.5	4.4	6	A0B
S037	11.0	330.0	1.5 - 3.5	4.4	6	A0B
S038	15.0	88.0	1.5 - 3.5	3.9	6	A0B
S039	10.0	95.0	1.5 - 3.5	3.9	6	A0B
S041	99999.9	0.0	2.0 - 4.0	4.4	9	A0AB
S042	10.2	30.0	2.0 - 4.0	4.4	9	A0AB
S043	10.2	90.0	2.0 - 4.0	4.4	9	A0AB
S044	10.2	150.0	2.0 - 4.0	4.4	9	A0AB
S045	10.2	210.0	2.0 - 4.0	4.4	9	A0AB
S046	10.2	270.0	2.0 - 4.0	4.4	9	A0AB
S047	10.20	330.0	2.0 - 4.0	4.4	9	A0AB
S048	15.0	88.0	2.0 - 4.0	3.9	9	A0AB
S049	10.0	95.0	2.0 - 4.0	3.9	9	A0AB
S051	99999.9	0.0	2.5 - 4.5	4.4	9	A0AB
S052	8.9	30.0	2.5 - 4.5	4.4	9	A0AB
S053	8.9	90.0	2.5 - 4.5	4.4	9	A0AB
S054	8.9	150.0	2.5 - 4.5	4.4	9	A0AB
S055	8.9	210.0	2.5 - 4.5	4.4	9	A0AB
S056	8.9	270.0	2.5 - 4.5	4.4	9	A0AB
S057	8.9	330.0	2.5 - 4.5	4.4	9	A0AB
S058	15.0	88.0	2.5 - 4.5	3.9	9	A0AB
S059	10.0	95.0	2.5 - 4.5	3.9	9	A0AB
S061	99999.9	0.0	3.0 - 5.0	4.4	9	A0AB
S062	10.5	30.0	3.0 - 5.0	4.4	9	A0AB
S063	10.5	90.0	3.0 - 5.0	4.4	9	A0AB
S064	10.5	150.0	3.0 - 5.0	4.4	9	A0AB
S065	10.5	210.0	3.0 - 5.0	4.4	9	A0AB
S066	10.5	270.0	3.0 - 5.0	4.4	9	A0AB
S067	10.5	330.0	3.0 - 5.0	4.4	9	A0AB
S068	15.0	88.0	3.0 - 5.0	3.9	9	A0AB
S069	10.0	95.0	3.0 - 5.0	3.9	9	A0AB
S071	99999.9	0.0	3.5 - 5.5	4.4	9	A0AB
S072	11.1	30.0	3.5 - 5.5	4.4	9	A0AB
S073	11.1	90.0	3.5 - 5.5	4.4	9	A0AB
S074	11.1	150.0	3.5 - 5.5	4.4	9	A0AB
S075	11.1	210.0	3.5 - 5.5	4.4	9	A0AB
S076	11.1	270.0	3.5 - 5.5	4.4	9	A0AB

Table 7.5.1. Spitsbergen beam table, valid from 1992/328 (23 November 1992). The table shows the name of the beam, velocity (km/sec), azimuth (degrees), filter band (Hz), STA/LTA threshold, and configuration. The configuration is described with number of sensors and a configuration code. Here, A0AB means center A0 SPZ plus A-ring plus B-ring, and A0B means A0 SPZ plus B-ring. SI01 - SI06 are incoherent beams using SPZ channels only. (Page 1 of 2)

S077	11.1	330.0	3.5 - 5.5	4.4	9	A0AB
S081	99999.9	0.0	4.0 - 8.0	4.4	9	A0AB
S082	9.5	30.0	4.0 - 8.0	4.4	9	A0AB
S083	9.5	90.0	4.0 - 8.0	4.4	9	A0AB
S084	9.5	150.0	4.0 - 8.0	4.4	9	A0AB
S085	9.5	210.0	4.0 - 8.0	4.4	9	A0AB
S086	9.5	270.0	4.0 - 8.0	4.4	9	A0AB
S087	9.5	330.0	4.0 - 8.0	4.4	9	A0AB
S091	99999.9	0.0	5.0 - 10.0	4.9	9	A0AB
S092	10.5	30.0	5.0 - 10.0	4.9	9	A0AB
S093	10.5	90.0	5.0 - 10.0	4.9	9	A0AB
S094	10.5	150.0	5.0 - 10.0	4.9	9	A0AB
S095	10.5	210.0	5.0 - 10.0	4.9	9	A0AB
S096	10.5	270.0	5.0 - 10.0	4.9	9	A0AB
S097	10.5	330.0	5.0 - 10.0	4.9	9	A0AB
S101	99999.9	0.0	8.0 - 9.0	4.9	9	A0AB
S102	9.9	30.0	8.0 - 9.0	4.9	9	A0AB
S103	9.9	90.0	8.0 - 9.0	4.9	9	A0AB
S104	9.9	150.0	8.0 - 9.0	4.9	9	A0AB
S105	9.9	210.0	8.0 - 9.0	4.9	9	A0AB
S106	9.9	270.0	8.0 - 9.0	4.9	9	A0AB
S107	9.9	330.0	8.0 - 9.0	4.9	9	A0AB
S201	99999.9	0.0	1.0 - 3.0	4.0	6	A0B
S207	99999.9	0.0	8.0 - 9.0	4.5	6	A0B
S254	99999.9	0.0	2.0 - 4.0	4.0	6	A0B
S282	99999.9	0.0	4.0 - 8.0	4.0	6	A0B
S310	99999.9	0.0	1.0 - 2.0	2.5	6	A0B
S312	99999.9	0.0	2.0 - 4.0	2.4	6	A0B
SI01	99999.9	0.0	0.5 - 1.5	3.2	6	A0B
SI02	99999.9	0.0	1.0 - 2.0	3.2	6	A0B
SI03	99999.9	0.0	1.5 - 2.5	3.0	6	A0B
SI04	99999.9	0.0	2.0 - 4.0	2.6	6	A0B
SI05	99999.9	0.0	3.5 - 5.5	2.6	6	A0B
SI06	99999.9	0.0	5.0 - 10.0	2.8	6	A0B

Table 7.5.1. (Page 2 of 2)

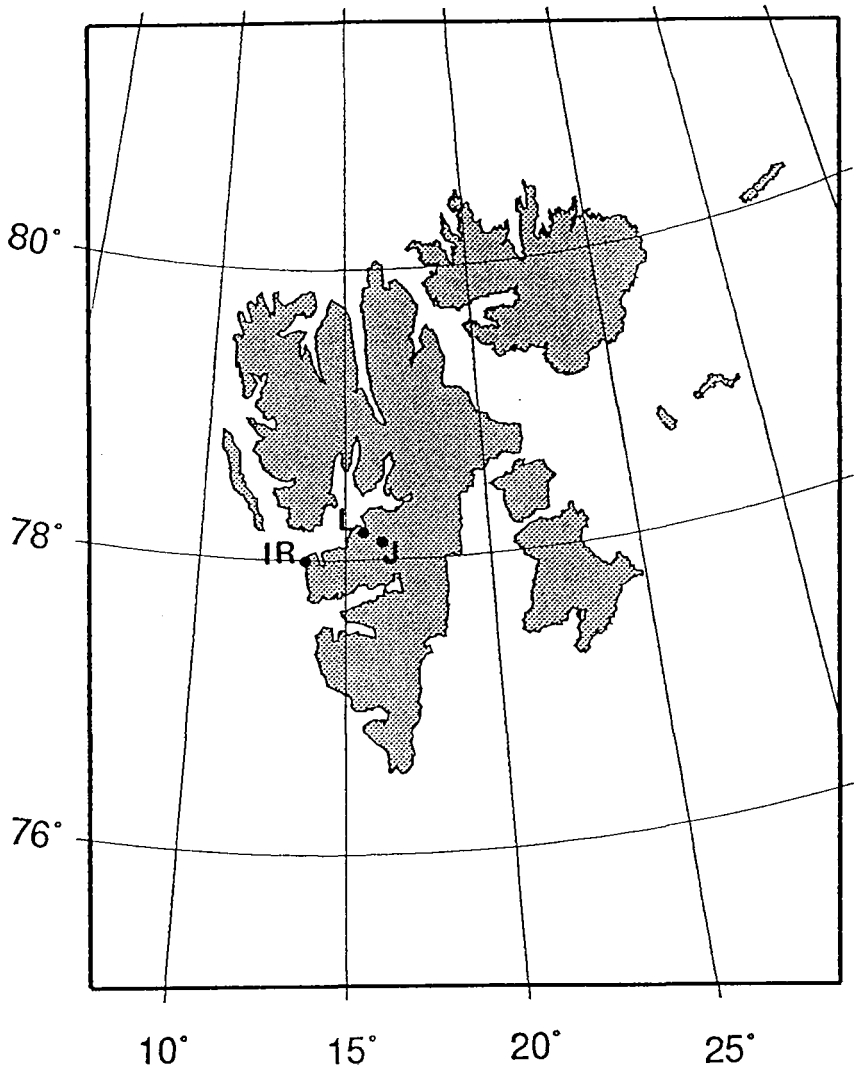

Fig. 7.5.1. This map of the Svalbard archipelago with its main island Spitsbergen shows the location of the array site at Janssonhaugen (J), the location of the array controller at Norwegian Telecom's facility at Longyearbyen (L), and the location of the NORSAT B earth station at Isfjord Radio (IR).

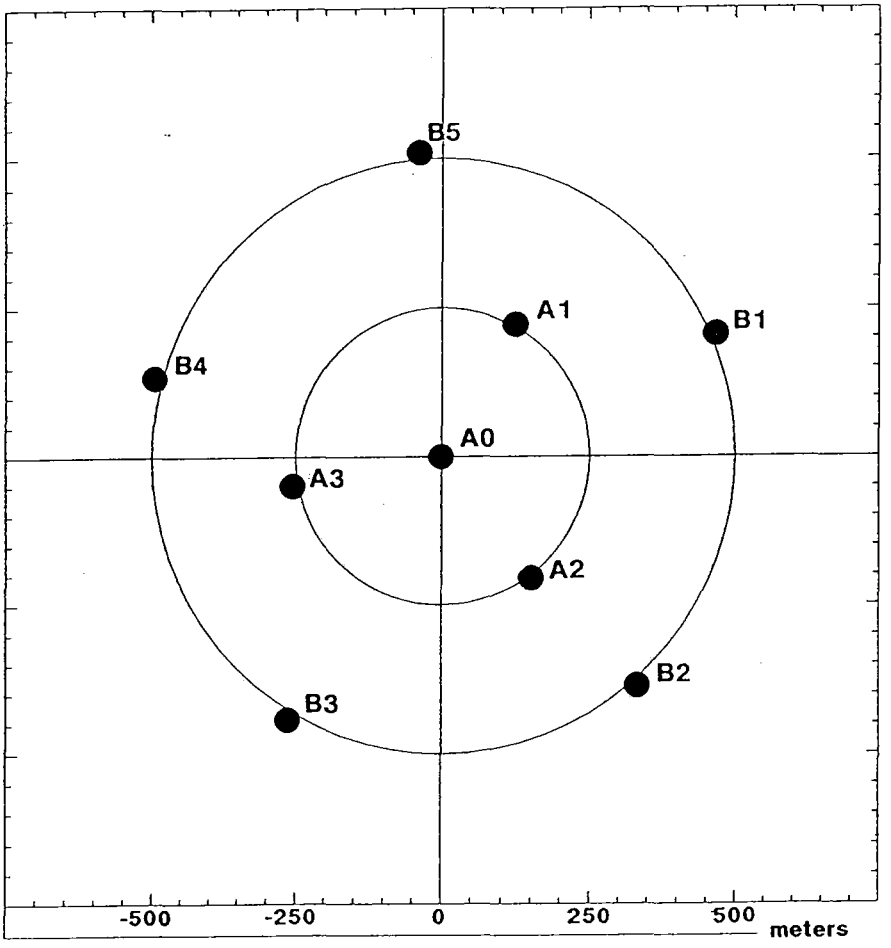

Fig. 7.5.2. Configuration of the new Spitsbergen small-aperture array.

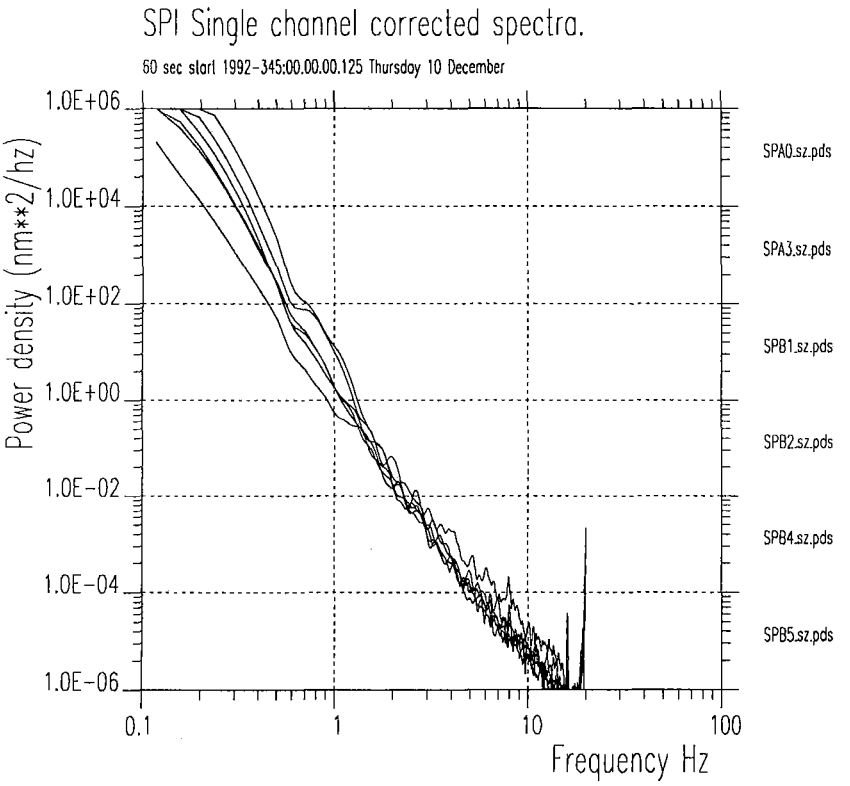

Fig. 7.5.3a. Noise spectra corrected for system response for the Spitsbergen array for 6 vertical channels. The spectra are based on one minute of data at 00.00 hours GMT on day 345, 1992. The power density is in nm^2/Hz.

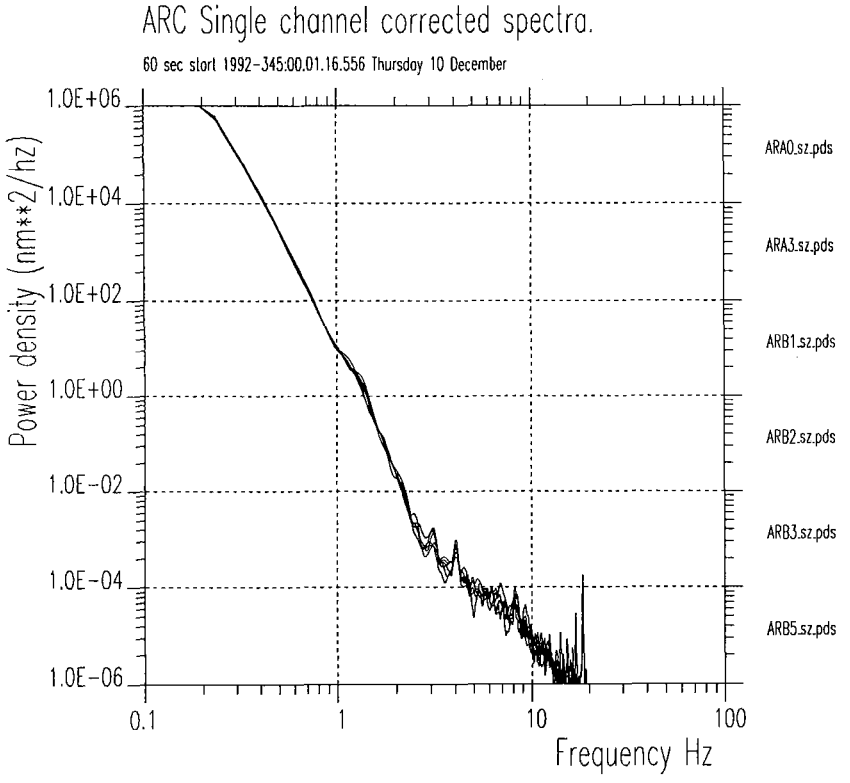

Fig. 7.5.3b. Same as Fig. 7.5.1a, but for ARCESS data taken at 00.00 hours GMT on day 345, 1992.

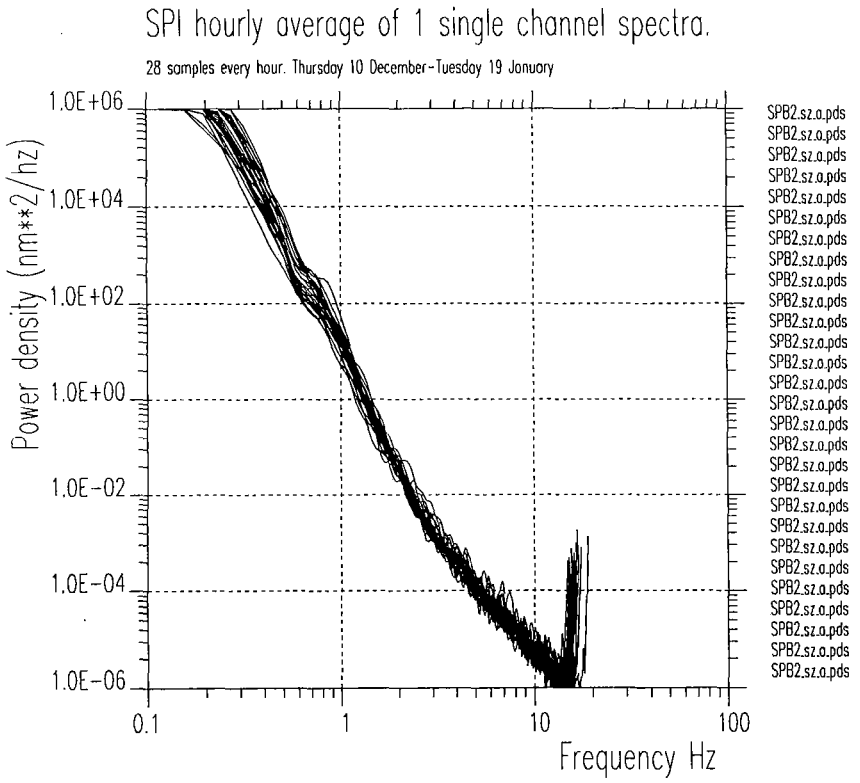

Fig. 7.5.4a. Corrected noise spectra for the Spitsbergen array for 41 one-minute intervals taken daily at 00.00 GMT from 10 December 1992 - 19 January 1993. Each spectrum represents data from the B2 SPZ seismometer.

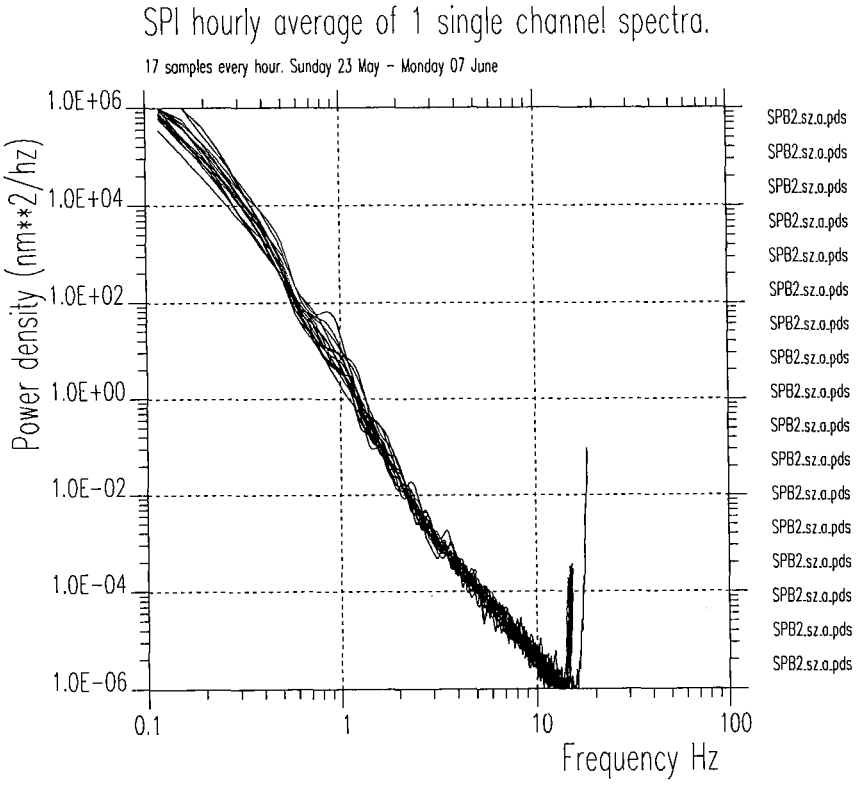

Fig. 7.5.4b. Same as Fig. 7.5.4a but for the time period 23 May - 7 June 1993.

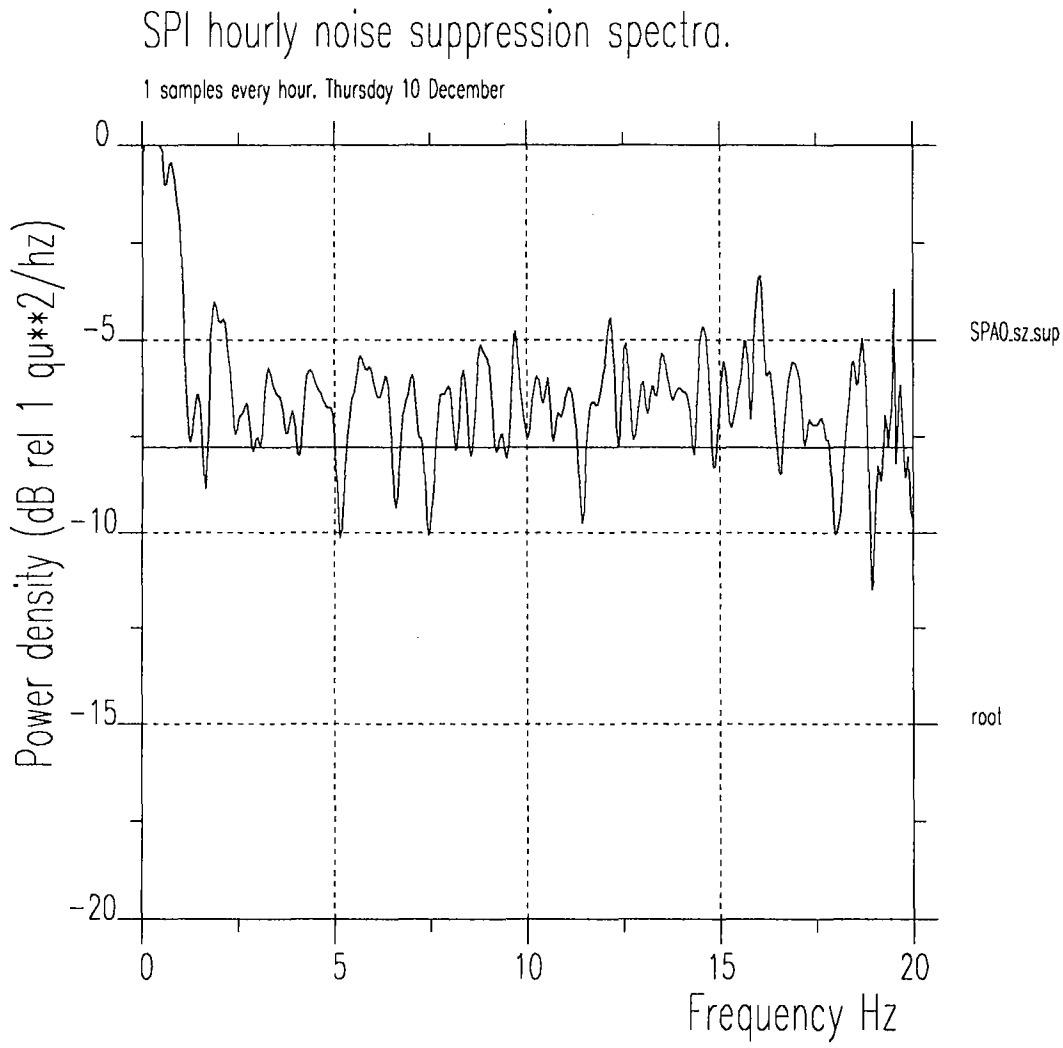

Fig. 7.5.5. Spitsbergen array noise suppression by beamforming for the initial geometry. The plot shows an average of 24 curves. To produce each of these curves, an infinite-velocity beam is formed and the spectrum for this beam is divided by the average of the single sensor spectra. The 24 curves result from one minute of data taken hourly between 00.00 and 23.00 hours GMT on day 345, 1992. The horizontal line at -8 dB represents $\sqrt{N}$ suppression for 6 sensors.

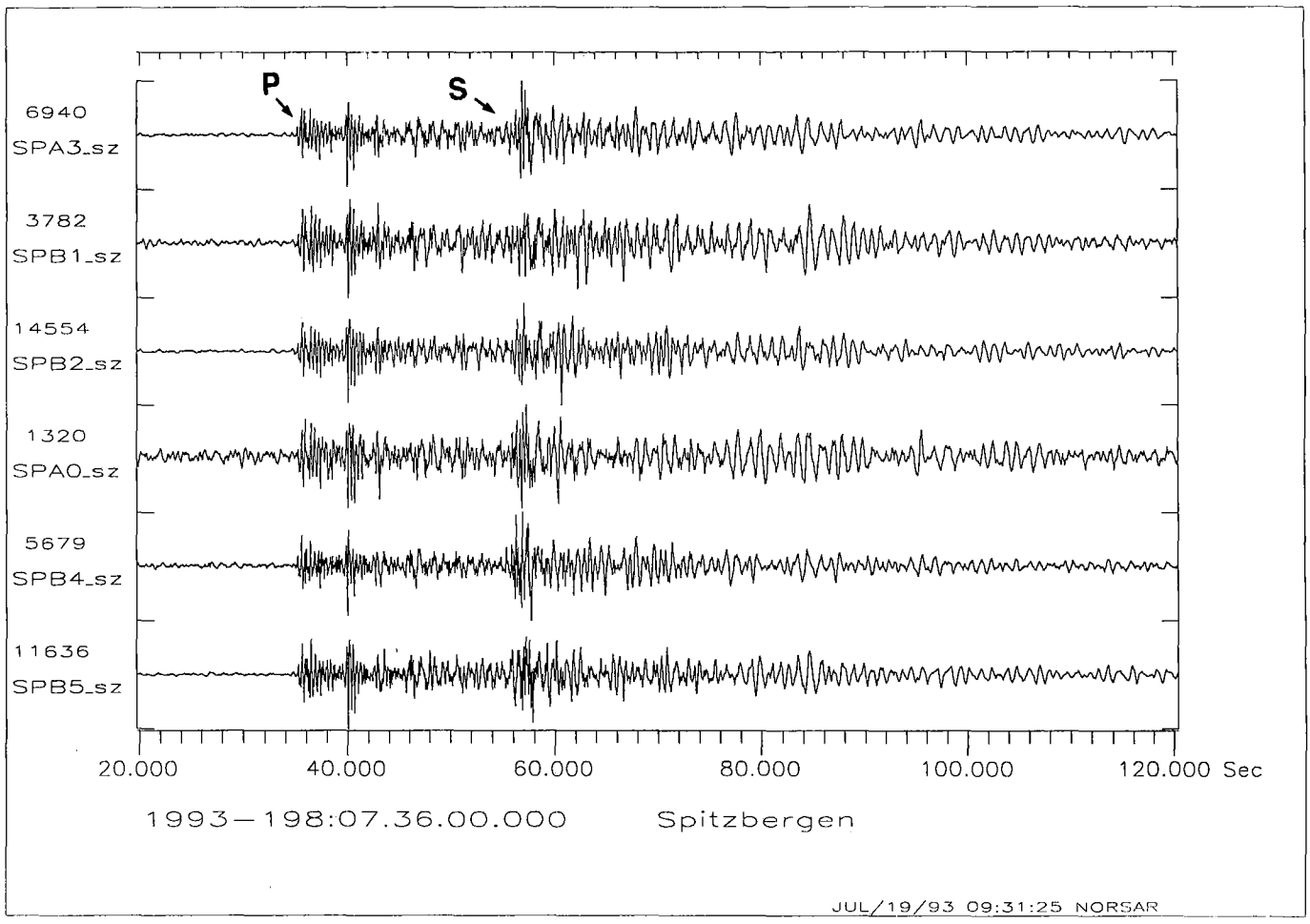

Fig. 7.5.6. Plot of individual Spitsbergen SPZ channels for the event discussed in the text. Note the very prominent amplitude variation across the array, as seen by the scale factors to the left of each trace.

a) P phase

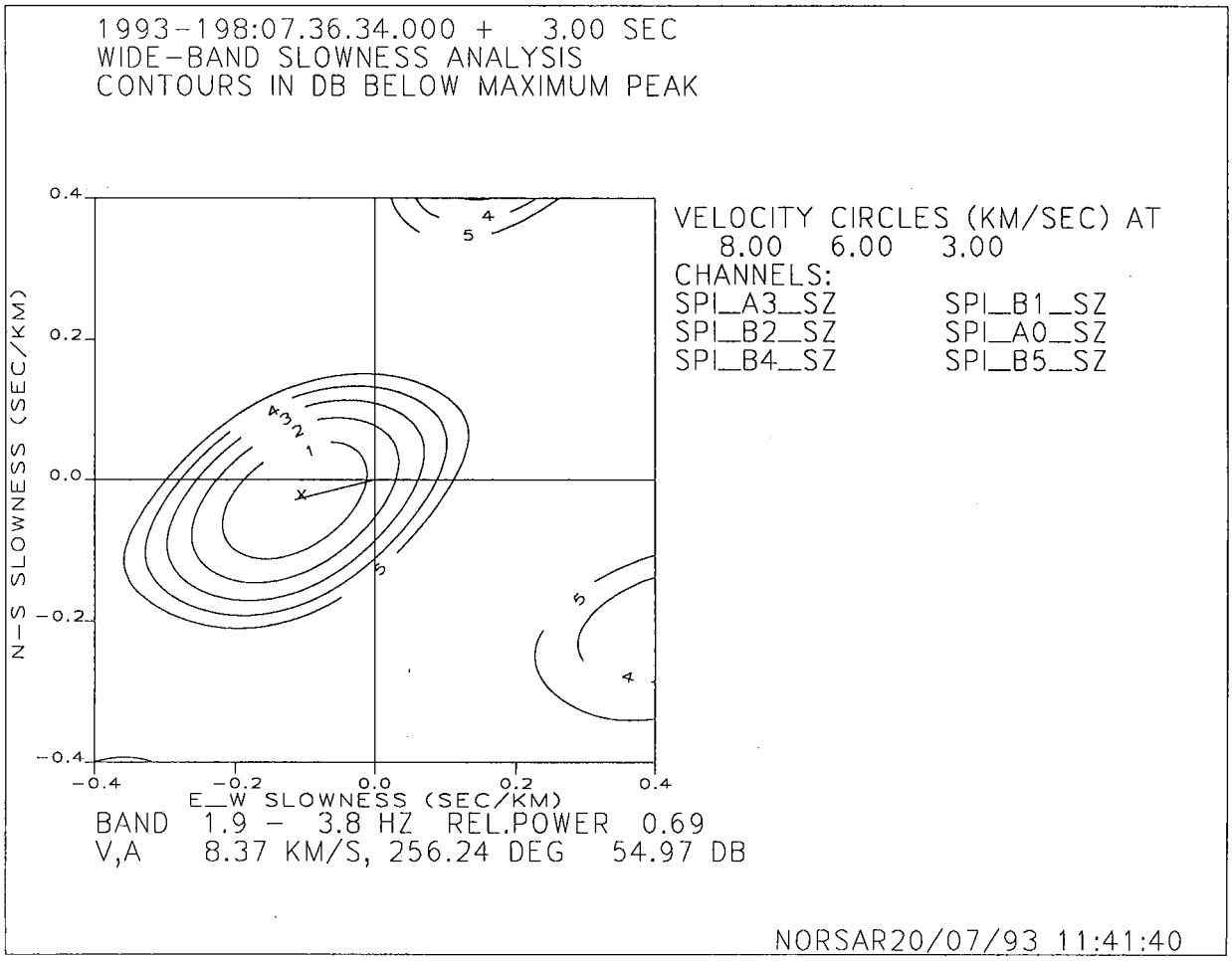

Fig. 7.5.7. Broadband F-K analysis results for the P and S phases of the event shown in Fig. 7.5.6. The figure shows a) the P phase, and b) the S phase. (Page 1 of 2).

b) S phase

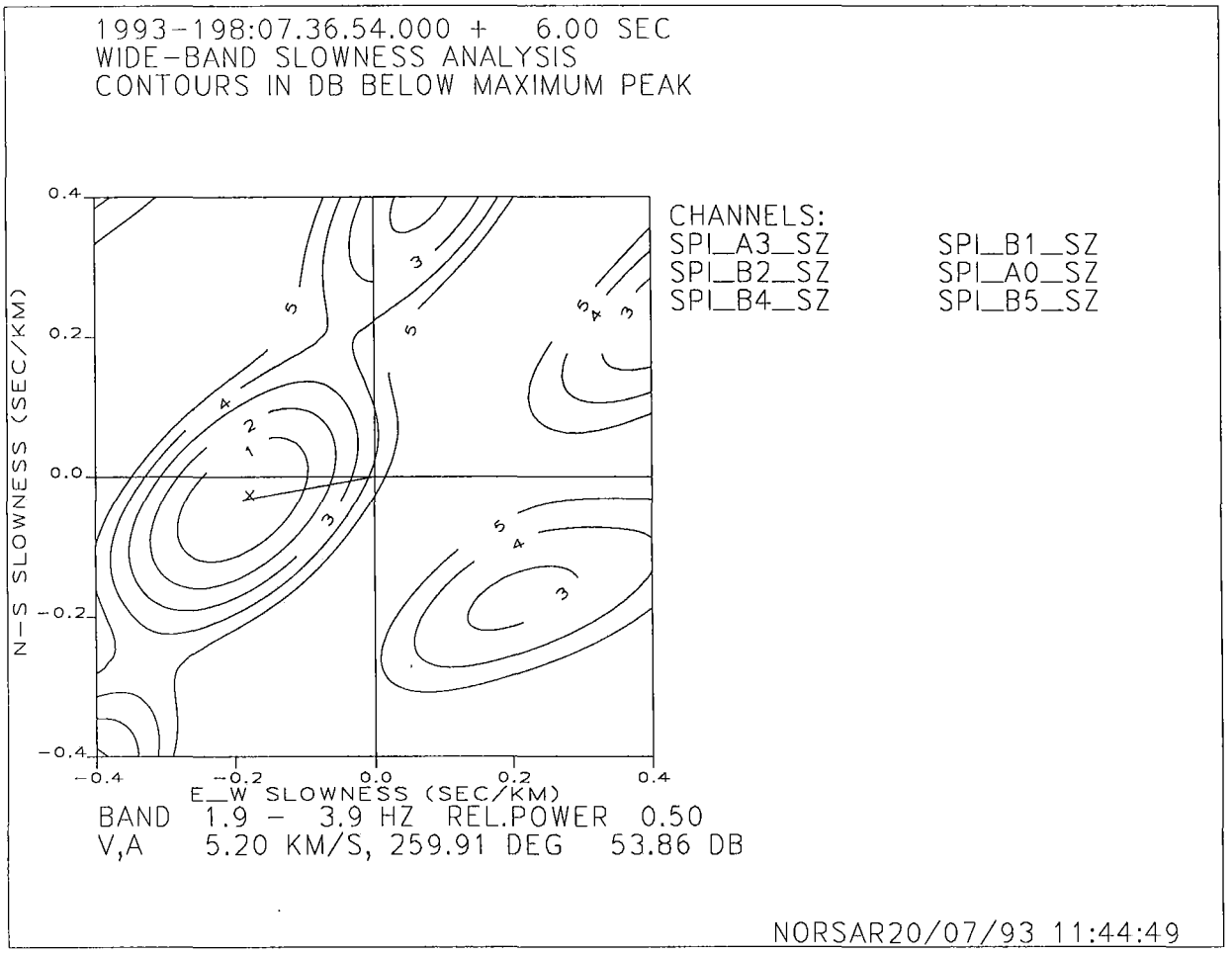

Fig. 7.5.7. (Page 2 of 2)